

Passive SAR Satellite System (PASSAT): Ground Trials

George M Atkinson, Alp Sayin, Mikhail Cherniakov,
Michael Antoniou, Andy Stove
Department of Electrical Engineering
University of Birmingham
Birmingham, UK
Email: m.antoniou@bham.ac.uk

Craig I Underwood
Surrey Space Centre
University of Surrey
Surrey, UK

Abstract — This paper presents progress made on the investigation of a passive Synthetic Aperture Radar (SAR) using digital terrestrial television broadcasting stations (DVB-T) as illuminators of opportunity, and micro-/nano-satellite receivers on Low Earth Orbit (LEO). The paper presents initial calculations on satellite payload requirements, describes the development of a passive SAR demonstrator to explore potential PASSAT image features, and describes an experimental campaign with a ground-moving vehicle to verify its functionality. The obtained SAR images are presented and discussed.

Keywords—Low earth orbit satellites, Passive Radar, Synthetic Aperture Radar, DVB-T

I. INTRODUCTION

Over the last decades space-borne Synthetic Aperture Radar (SAR) has proved its capability as a remote sensing technique of great power and value over a plethora of applications[1]–[3]. However, these very capable orbital systems come with a high system complexity and cost, which restrict the number of instruments that can be built in practice. This is in contrast to increasing demands for persistent or near-persistent monitoring applications, which require a large number of SAR satellites to achieve.

One potential solution to this problem could be to have passive, rather than active, space-borne SAR systems, which reuse existing transmissions from other sources (e.g. communication systems) for imaging purposes. One such system is the Passive SAR Satellite constellation (PASSAT) concept[4]. In this system, transmitters of opportunity are ground-based broadcasting stations, presumably Digital Video Broadcasting – Terrestrial (DVB-T), while the receivers are on-board satellites in Low Earth Orbit LEO (Fig. 1).

A generic passive radar concept combining space-borne and ground-based segments is not entirely new. For example, passive SAR with navigation satellites as transmitters and ground-based receivers has been considered at length in a number of publications[5]–[10]. This is essentially the opposite configuration from PASSAT (where now we have a single transmitter on the ground and multiple receivers in space), where a number of key issues directly applicable to this concept

(such as image formation or multi-static operation) have already been considered. In other work, the German Aerospace Centre (DLR) has considered a constellation of receive-only LEO satellites, with a satellite in geostationary orbit acting as the transmitter[11].



Fig. 1: The PASSAT concept

However, placing the receiver in space and using a transmitter on the ground introduces a number of new features at the engineering and scientific levels. First of all, since the satellites are receive-only, micro-/nano-satellite platforms (CubeSat standards) may be used that drastically reduce system costs. For the same reason, a number of satellites can be launched as part of a SAR constellation to provide very small times between image updates or even persistent monitoring in areas where there is DVB-T coverage (e.g. in the UK nearly 90% of the country is within DVB-T coverage, not to mention littoral waters[12]). At the same time, the combination of DVB-T signal characteristics with bistatic acquisition geometries could enhance image information space, making such a system able to operate on its own as well as to complement existing SAR instruments. A single DVB-T multiplex has a sufficiently wide signal bandwidth (~8MHz) for Earth Observation, and a transmit power up to hundreds of kilowatts. In addition, DVB-T operates in the VHF/UHF region, which is known for features such as foliage penetration and indirect propagation, whereas

conventional orbital SARs operate in the L- to X-band. Bistatic operation takes advantage of bistatic scattering effects and shadow reduction to offer further scene information.

However, as a new concept, the appropriate feasibility study should be done to confirm its validity and explore its potential, which is being aided by the fact that DVB-T SAR is fundamentally possible, as recent proof-of-concept results have shown[13]–[16].

In a recent paper, preliminary calculations on the system sensitivity, resolution, and robustness to unfavourable imaging geometries were made[17]. In this paper, we will describe the next step in the study of this system, which has focused on deriving requirements for the PASSAT space segments, as well as the development of a DVB-T SAR technology demonstrator, its validation through an experimental campaign with a moving ground vehicle platform, and a first analysis of the results obtained. This step is a springboard for the development of an airborne demonstrator which will study the expected image properties and features of PASSAT.

The paper is organized as follows: Section II presents preliminary considerations on the PASSAT space segment, Section III presents the experimental campaign carried out with the technology demonstrator, and Section IV shows and discusses experimental images obtained.

II. FIRST SPACE SEGMENT REQUIREMENTS ANALYSIS

Table 1 below shows some major PASSAT parameters, from which some first conclusions on the requirements of the space segment can be drawn.

Table 1: PASSAT major parameters

Parameter	Value
Effective Radiated Power (ERP)	100 kW
Radar wavelength	0.46m
Signal bandwidth (single DVB-T channel)	7.61 MHz
Receive antenna gain	15 dB
Receiver noise figure	5 dB
Receiver altitude	400km
Receiver orbital speed	7672 m/s

An ERP of 100 kW is taken as a typical value for DVB-T broadcasting stations. A radar wavelength of 0.46m corresponds to an operating frequency of approximately 650 MHz, which sits within of the DVB-T allocated spectrum. The choice for the receive antenna gain is the result of a trade-off between a favourable power budget and a resulting antenna size that could be fitted within a nano-satellite, to yield a favourable sensitivity. The orbital altitude should be below that of the International Space Station (ISS) to ensure the latter’s safety, hence the value given for the satellite altitude.

To begin our considerations on the requirements for the satellite segment, let us assume as a starting point that PASSAT requires, as a minimum, that a VHF/UHF receiver be flown that can store samples of the signals received over an 8 MHz bandwidth during a dwell time on target of at least 80 seconds, which would give an azimuth resolution of a few meters [17]. It is also assumed that SAR data are downloaded to the station without any image formation processing done on-board the satellite as the worst case scenario in terms of data rates and volumes, and that a typical pass time over a ground station in the UK is approximately 10mins. Assuming 8-bits per sample, and 16 MHz sampling rate, this requires approximately 1.2 Gbyte of on-board data storage. This could easily be accommodated using flash memory storage. The receiver itself is no different to a UHF super-heterodyne receiver and can therefore be very compact. From that perspective, it is envisaged that the receiver/data storage element could be accommodated in a “1U” (approximately 10cm x 10cm x 10cm) volume of a “12U” CubeSat-type spacecraft, which has approximate dimensions 20cm x 20cm x 30cm.

Based on the calculations above, to download the signal sample data in a single pass, a downlink data rate of approximately 18 Mbps would be required – assuming a 10% data packet overhead. Lossless data compression could reduce this by a factor of 3 (6 Mbps), which would bring the data rate into the range available using the S-band high-rate transmitter (up to 10 Mbps) made by Surrey Satellite Technologies Ltd, with a size of 200 x 191 x 80 mm, and a mass of 1.8 kg [4]. It should therefore be just about possible to accommodate it in a bespoke 12U CubeSat structure – leaving enough room for the rest of the spacecraft sub-systems, payload receiver and deployable antenna. If a slightly more capable payload becomes necessary, of course a slightly larger platform could be used, but still based on the CubeSat concept. If the images are formed on the satellite they could be subject to lossy data compression to ~1bit/sample and the resulting 2 Mbps would be just about feasible which just brings the data-rate into the realm of a CubeSat S-band downlink transmitter.

The data downlink is therefore one of the main engineering challenges for the mission, and this will need further study as the mission and payload characteristics are refined, as well as the amount of signal processing to be carried out on-board the satellite. The usual CubeSat VHF or UHF downlink transmitters, operating at 9600 bps or 38,400 bps, would not be able to support the required payload data downlink – however, such transmitters could still be carried as a back-up, and to provide normal platform telemetry.

The peak power demand of the payload and downlink transmitter would be ~6 -10W for no more than 10 minutes, which is well within the capability of a 12U CubeSat. A simple “rule-of-thumb” metric is that for typical LEO missions, the orbit average power in watts is numerically equal to the mass of the spacecraft in kg (12-15kg for a 12U CubeSat) for body mounted solar arrays. Deployed arrays can increase this, but add complexity.

It has been determined that helical antenna of approximately 10 turns should be used as the DVB-T 15dB gain receiving antenna, as this design has the added benefit of circular polarization to overcome the deep fading effect due to Faraday rotation in the ionosphere[4]. For DVB-T frequencies, the antenna would need to be 1.2m in length, and so must be deployable from the CubeSat. Such an antenna would have a 20-degree 3dB beam-width, and would fit within a 4U volume of the satellite. A prototype of a deployable helical antenna is currently in development at Surrey Space Centre.

The CubeSat can be orientated through the use of a pitch momentum wheel and a yaw reaction wheel, along with dual redundant 3-axis magnetorquers as actuators. These systems allow the satellite to maintain a pointing stability to within $\pm 0.5^\circ$. For orbital control, a butane propellant based propulsion system, providing 5-10 mN of thrust would be used. A 1.5U volume of the CubeSat would be required to hold the propellant. The position of the satellite is known to a relatively high precision (approximately ± 15 m) through the use of an on-board multi-channel GNSS receiver, which also provides a timing reference.

Combining all the elements above together, the conclusion of the space segment analysis is that the mission should be feasible with a 12U CubeSat type platform (approximately 2U for avionics, 1.5U for propulsion, 1U for the receiver payload, 3U for the S-Band downlink and 4U for the stowed deployable antenna).

III. PASSIVE SAR EXPERIMENTAL CAMPAIGN

A series of road trials were conducted to obtain DVB-T data sets for the production of passive SAR imagery. The latest successful measurements at the time of writing had been taken in January 2018. Bartley Reservoir, close to the University of Birmingham, was chosen as a location as it presented a near quasi-monostatic geometry, as well as a straight road to provide a linear aperture. Figure 2 shows an aerial view of Bartley Reservoir, with the vehicle path shown in yellow, the imaging direction indicated by the green arrow, and the direction to the Sutton Coldfield transmitter is indicated by the red lines.



Fig. 2. Image of the Bartley Reservoir road, with the aperture track shown in yellow, the imaging direction in green, and the direction to the Sutton

The Sutton Coldfield transmitting station was used as the DVB-T transmitter of opportunity for these measurements. This transmitter has a height of 433 m above sea level and, for the 650MHz carrier frequency, an ERP of 200 kW. The transmitter is located 21.63 km from the centre of the aperture, at an angle of 73 degrees from the direction of motion of the receiver. The full length of the road is 500m, however, for a typical measurement a roughly 400m aperture was produced in which the vehicle was travelling at a relatively constant speed of 20m.ph (about 9ms^{-1}) for approximately 40 seconds per measurement.

The receiver was mounted on the University of Birmingham's mobile laboratory, a Land Rover Discovery (Fig.3).



Fig. 3. Land Rover Discovery vehicle used for ground-based measurements, with two patch antennas mounted on 1.5 long poles atop the roof of the car.

The receiver was based on a Universal Software Radio Peripheral (USRP), made by National Instruments. Two receiving channels were used, one to capture the direct DVB-T signal and one for radar echo reception. The receiving antennas were patch antennas with a 50° beam-width, custom-made at the University of Birmingham for ultimate installation within an airborne platform. The antennas are followed by band-pass filters for interference rejection. The antennas were mounted on 1.5m poles atop the mobile laboratory, placing them a total of 3m above ground level. The USRP streamed I and Q samples from both channels to a laptop computer. Simultaneously to the radar measurement, a high precision SpatialFog Inertial Measurement Unit (IMU) and GPS record the position of the vehicle with a high update rate. The SpatialFog unit was connected to the same control laptop as the USRP and the position data was recorded to the same SSD. The IMU, USRP and antenna front-ends were mounted securely within a vibration-resistant box, along with batteries to provide power. This is necessary for future experiments that will involve their carriage in a small aircraft.



Fig. 4. Aerial image of Bartley Reservoir overlaid with the GPS position track, shown in pink.

Table 2: Parameters for target scene and transmitter

Total Track Length	500 m
Synthetic Aperture Length	~400 m
Receiver Centre Frequency	650 MHz
Receiver Bandwidth	10 MHz
Distance to Transmitter (at aperture centre)	21.63 km
Angle to Transmitter (at aperture centre)	73°

IV. EXPERIMENTAL RESULTS AND DISCUSSION

The results shown here are from a single measurement, with the receiver travelling in the direction shown by the yellow arrow in figure 2. A back-projection algorithm was used to produce the SAR imagery for this measurement on a pulse by pulse basis. Range compression was performed by cross-correlating the reference and radar channels from the recorded data.

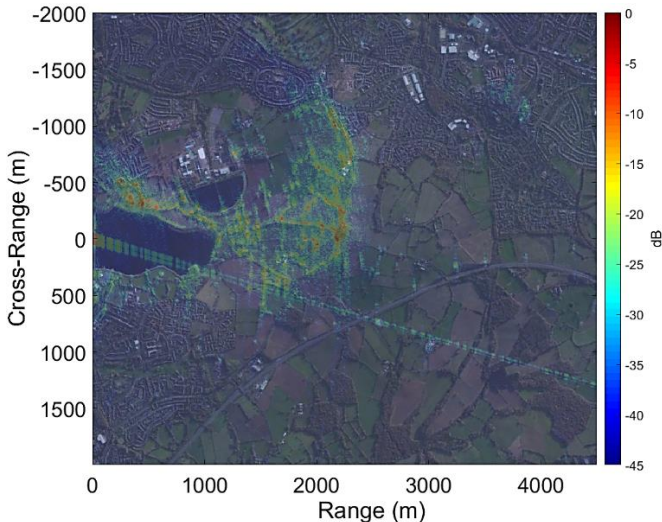


Fig. 5. Reconstructed SAR image of Bartley Reservoir target scene from road measurements, overlaid with ground-truth satellite imagery.

Figure 5 shows an image generated from this measurement, with a ground truth satellite image overlay. The area imaged is 4km in cross-range and 5km in range, spanning a total area of 20km squared. The colour scale is in dB, with 0dB representing the highest echo intensity in the image. The image is also plotted on a local reference frame, where the origin is at the receiver location at the midpoint of the aperture. It is stated here that at a 21km distance the transmitter is at near-grazing, while the receiver is a ground vehicle, so it is also at near-grazing. In a high-frequency SAR, we would expect the front face of targets at near range to be imaged, with large parts of the target area behind them in shadow. However, such an effect is not shown here. On the contrary, the image looks more similar to that of an airborne SAR system, with typical grazing angles around 20 degrees, rather than a ground-based SAR. This is credited to the indirect propagation effects that low-frequency radar systems possess.

Immediately obvious are the strong returns at zero range and a repeating pattern of strong returns across the image. These returns are due to the main-lobe and side-lobe detection of a wall that runs parallel to the road used, with an approximate height of 2m. While the mounting of the antennas atop long poles attempted to mitigate these returns, the wide antenna beam-width combined with the proximity to the wall made them unavoidable.

Also notable in the image, when overlaid with the ground truth image, is that the main reservoir, and the smaller reservoir, are clearly outlined. A walkway that runs across the smaller, semi-circular, reservoir is clearly visible in the image, shown more closely in figure 9. Careful inspection of the image reveals that many of the strong returns are from trees, bushes and forested areas. Along the road towards the bottom of the image can be seen a series of strong, almost point-like, returns which, after inspection of ground-truth, are from a series of electricity pylons running parallel to a motorway.

Gaps in the resulting image, where no returns are visible beyond a range of ~2500 m, despite being within the antenna main lobe, can partially be explained by the terrain. Figure 6 shows the SAR image overlaid the ground-truth and then mapped to a 3D topological map of the scene, where the z-axis represents the vertical height of the terrain map, relative to sea level. The presence of a large hill, approximately 80m higher than the road level at the highest point, goes towards explaining why large areas behind the hill are not visible to the receiver. The exception to this being a set of three high-rise buildings, shown more closely in figure 7, and the pylons follow the motorway, shown in figure 9. It is crucial to highlight here that while the high-rise buildings may or may not be taller than the height of the hill, the pylons certainly are not. This is another preliminary, but encouraging result showing the potential of the system for “beyond the hill” vision.

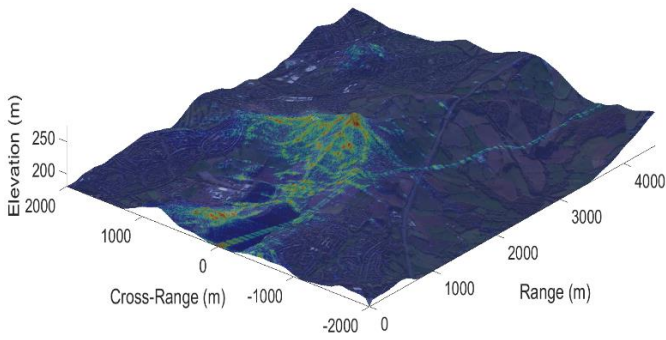


Fig. 6. Topographic map of the Bartley Reservoir area, overlaid with a satellite image of the area and the SAR image shown in fig. 5.



Fig. 7. Subsection of the SAR image shown in figure 5. (a) SAR image of an area surrounding three high-rise buildings (highlighted by red outline) overlaid with a satellite image of the area. (b) Satellite image of the area shown in (a).

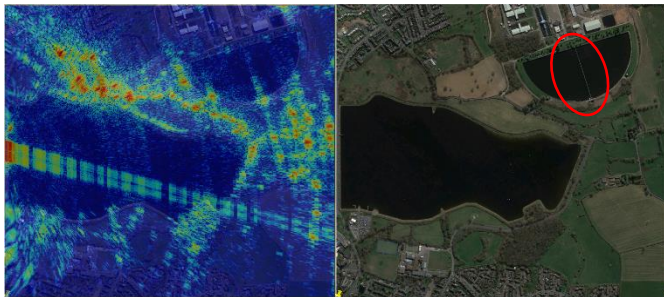


Fig. 8. Subsection of the SAR image shown in figure 5. (a) SAR image of an area around Bartley Reservoir overlaid with a satellite image of the area. (b) Satellite image of the area shown in (a) with walkway over smaller reservoir shown by red outline.



Fig. 9. Subsection of the SAR image shown in figure 5. (a) SAR image of an area around a series of electricity pylons, overlaid with a satellite image of the area. (b) Satellite image of the area shown in (a) electricity pylons highlighted by red circles.

V. CONCLUSIONS AND FUTURE WORK

This paper reports current progress in the development of the PASSAT concept. In terms of the satellite mission, preliminary calculations on payload requirements show that a 12U CubeSat is feasible, but further research is required on the data downlink and the deployable antenna, which is currently underway. Regarding the SAR subsystem, a technology demonstrator was built and tested using a ground moving vehicle. The experiments not only confirm the functionality of the system, but also start to indicate expected outcomes of the overall technology such as indirect propagation effects. The next step is to move from ground vehicle trials to airborne trials to better explore potential PASSAT image features.

REFERENCES

- [1] S. Buckreuss, R. Werninghaus, and W. Pitz, "The German satellite mission TerraSAR-X," *IEEE Aerosp. Electron. Syst. Mag.*, vol. 24, no. 11, pp. 4–9, Nov. 2009.
- [2] R. Raney, "RADARSAT-Canada's national radar satellite program," *IEEE Antennas Propag. Soc. Newsl.*, vol. 25, no. 3, pp. 4–8, Jun. 1983.
- [3] M. Virelli, A. Coletta, and M. L. Battagliere, "ASI COSMO-SkyMed: Mission Overview and Data Exploitation," *IEEE Geosci. Remote Sens. Mag.*, vol. 2, no. 2, pp. 64–66, Jun. 2014.
- [4] C. I. Underwood, M. Cherniakov, M. Antoniou, M. Gashinova, and A. Stove, "PASSAT: Passive imaging radar constellation for near-persistent Earth Observation," presented at the 11th IAA conference on small satellites for Earth Observation, 2017.
- [5] M. Antoniou, M. Cherniakov, and C. Hu, "Space-Surface Bistatic SAR Image Formation Algorithms," *IEEE Trans. Geosci. Remote Sens.*, vol. 47, no. 6, pp. 1827–1843, Jun. 2009.
- [6] M. Antoniou, Z. Zeng, L. Feifeng, and M. Cherniakov, "Experimental Demonstration of Passive BSAR Imaging Using Navigation Satellites and a Fixed Receiver," *IEEE Geosci. Remote Sens. Lett.*, vol. 9, no. 3, pp. 477–481, May 2012.
- [7] H. Ma, D. Tzagkas, M. Antoniou, and M. Cherniakov, "Maritime Moving Target Indication and localisation with GNSS-based multistatic radar: Experimental proof of concept," in *2017 18th International Radar Symposium (IRS)*, 2017, pp. 1–10.
- [8] H. Ma *et al.*, "Maritime target detection using GNSS-based radar: Experimental proof of concept," in *2017 IEEE Radar Conference (RadarConf)*, 2017, pp. 0464–0469.
- [9] Q. Zhang, M. Antoniou, W. Chang, and M. Cherniakov, "Spatial Decorrelation in GNSS-Based SAR Coherent Change Detection," *IEEE Trans. Geosci. Remote Sens.*, vol. 53, no. 1, pp. 219–228, Jan. 2015.
- [10] M. Cherniakov and A. Moccia, Eds., *Bistatic radar: emerging technology*. Chichester: Wiley, 2008.
- [11] G. Krieger, H. Fiedler, D. Houman, and A. Moreira, "Analysis of system concepts for bi- and multi-static SAR missions," in *IGARSS 2003. 2003 IEEE International*

Geoscience and Remote Sensing Symposium. Proceedings (IEEE Cat. No.03CH37477), 2003, vol. 2, pp. 770–772 vol.2.

[12] “Digital UK | Multiplexes.” [Online]. Available: <http://www.digitaluk.co.uk/operations/multiplexes>. [Accessed: 12-Feb-2018]

[13] D. Gromek, K. Kulpa, and P. Samczyński, “Experimental Results of Passive SAR Imaging Using DVB-T Illuminators of Opportunity,” *IEEE Geosci. Remote Sens. Lett.*, vol. 13, no. 8, pp. 1124–1128, Aug. 2016.

[14] L. M. H. Ulander, P. O. Fröling, A. Gustavsson, R. Ragnarsson, and G. Stenström, “Airborne passive SAR imaging based on DVB-T signals,” in *2017 IEEE International Geoscience and Remote Sensing Symposium (IGARSS)*, 2017, pp. 2408–2411.

[15] L. M. H. Ulander, P. O. Fröling, A. Gustavsson, R. Ragnarsson, and G. Stenström, “VHF/UHF bistatic and passive SAR ground imaging,” in *2015 IEEE Radar Conference (RadarCon)*, 2015, pp. 0669–0673.

[16] P. O. Fröling, “Results of airborne passive SAR ground and sea target imaging using DVB-T signals,” in *2016 IEEE Radar Conference (RadarConf)*, 2016, pp. 1–4.

[17] H. Ma, A. G. Stove, G. Atkinson, C. I. Underwood, M. Cherniakov, and M. Antoniou, “Passive SAR Using Small Satellite Receivers for Persistent Earth Observation,” presented at the IET Radar 2017, Belfast, 2017.